





# Immunohistochemical Markers in the Diagnosis of Calcifying Pseudoneoplasm of the Neuraxis

Kaiyun Yang , Kesava Reddy, Bill H. Wang , Aleksa Cenic, John Provias, Snezana Popovic, William H. Yong, France Berthelet, Michel W. Bojanowski, Robert Hammond , Jian-Qiang Lu 

**ABSTRACT: Background:** Calcifying pseudoneoplasm of the neuraxis (CAPNON) is a rare tumor-like lesion with unknown pathogenesis. It is likely under-reported due to diagnostic challenges including the nonspecific radiographic features, lack of diagnostic markers, and often asymptomatic nature of the lesions. **Methods:** We performed detailed examination of 11 CAPNON specimens diagnosed by histopathology, with the help of electron microscopy and immunohistochemistry. **Results:** Electron microscopy revealed the presence of fibrillary materials consistent with neurofilaments. In addition to some entrapped axons at the periphery of CAPNONs, we discovered that all specimens stained positive for neurofilament-light (NF-L) within the granular amorphous cores, but not neurofilament-phosphorylated (NF-p). CAPNONs also showed variable infiltration of CD8+ T-cells and a decreased ratio of CD4/CD8+ T-cells, suggesting an immune-mediated process in the pathogenesis of CAPNON. **Conclusion:** NF-L and CD4/CD8 immunostains may serve as diagnostic markers for CAPNON and shed light on its pathogenesis.

**RÉSUMÉ :** Recourir à des marqueurs immunohistochimiques pour le diagnostic de pseudo-tumeurs calcifiantes du névraxe. **Contexte :** Les pseudo-tumeurs calcifiantes du névraxe (PTCN) sont des lésions rares ressemblant à des tumeurs dont la pathogénèse reste inconnue. On a probablement tendance à moins les signaler en raison d'écueils diagnostiques, par exemple des caractéristiques radiographiques non-spécifiques, un manque de marqueurs diagnostiques et la nature fréquemment asymptomatique de ces lésions. **Méthodes :** C'est à l'occasion d'un examen histopathologique, plus précisément au moyen de la microscopie électronique et de marqueurs immunohistochimiques, que nous avons effectué une analyse approfondie de 11 échantillons de PTCN. **Résultats :** La microscopie électronique a révélé la présence de matériaux fibrillaires (*fibrillary materials*) compatibles avec des neurofilaments. Outre certains axones piégés à la périphérie des PTCN, nous avons découvert que tous les échantillons, une fois soumis à la lumière de neurofilament, se sont déclarés positifs à l'intérieur de noyaux amorphes granulaires, ce qui n'a pas été le cas avec des neurofilaments phosphorylés. Les PTCN ont également donné à voir des infiltrations variables de lymphocytes T cytotoxiques possédant la protéine CD8 (*CD8 + T-cells*) et une diminution du ratio de lymphocytes T cytotoxiques possédant les protéines CD4 et CD8, ce qui suggère un processus d'origine immunitaire dans la pathogénèse des PTCN. **Conclusion :** L'immunocoloration des neurofilaments et des lymphocytes T cytotoxiques possédant les protéines CD4 et CD8 pourrait servir de marqueurs diagnostiques pour les PTCN et permettre ainsi de faire la lumière sur leur pathogénèse.

**Keywords:** Calcifying pseudoneoplasm of the neuraxis, Biomarkers, Neurofilaments, CD8, CD4, Immunohistochemistry, Diagnosis, Pathogenesis

doi:10.1017/cjn.2020.175

Can J Neurol Sci. 2021; 48: 259–266

## INTRODUCTION

Calcifying pseudoneoplasm of the neuraxis (CAPNON) is thought to be a rare tumor-like lesion that can occur anywhere in the neuraxis, including the brain, spinal cord, meninges, and their adjacent tissue. Since CAPNON was first characteristically described in 1978,<sup>1</sup> more than 100 cases have been

reported in the literature.<sup>2–4</sup> However, its prevalence is likely underestimated, since CAPNONs could be an incidental finding in asymptomatic patients.<sup>4</sup> In addition, its radiological features are nonspecific.<sup>3–8</sup> CAPNON is diagnosed exclusively by pathological examination in the form of a fibro-osseous lesion with the following histopathological features: granular

From the Department of Neurosurgery, University of Toronto, Toronto, Ontario, Canada (KY); Division of Neurosurgery, Department of Surgery, McMaster University, Hamilton, Ontario, Canada (KR, BHW, AC); Neuropathology Section, Department of Pathology and Molecular Medicine, McMaster University, Hamilton, Ontario, Canada (JP, JQL); Anatomic Pathology, Department of Pathology and Molecular Medicine, McMaster University, Hamilton, Ontario, Canada (SP); Division of Neuropathology, Department of Pathology and Laboratory Medicine, David Geffen School of Medicine at UCLA, Los Angeles, CA, USA (WHY); Department of Pathology and Cellular Biology, University of Montreal, Montreal, Quebec, Canada (FB); Division of Neurosurgery, Department of Surgery, University of Montreal, Montreal, Quebec, Canada (MWB); and Department of Pathology and Laboratory Medicine, Western University, London, Ontario, Canada (RH)

RECEIVED MAY 22, 2020. FINAL REVISIONS SUBMITTED JULY 12, 2020. DATE OF ACCEPTANCE AUGUST 5, 2020.

Correspondence to: Kaiyun Yang, MD, PhD, Department of Neurosurgery, University of Toronto 399 Bathurst Street, West Wing 4-427, Toronto, ON, Canada M5T 2S8. Email: [kaiyun.yang@medportal.ca](mailto:kaiyun.yang@medportal.ca); Jian-Qiang Lu, MD, PhD, FRCPC, Neuropathology Section, Department of Pathology and Molecular Medicine, McMaster University, Hamilton General Hospital, 237 Barton Street, Hamilton, Ontario, Canada L8L 2X2. Email: [luj85@mcmaster.ca](mailto:luj85@mcmaster.ca)

amorphous confluent cores with calcification/ossification, peripheral palisading spindle to epithelioid cells, variable fibrous stroma, and foreign-body reaction with multinucleated giant cells.<sup>3–6,9,10</sup> However, these histopathological features are variable and nonspecific as they may overlap with some other disease entities.<sup>3–11</sup> Although a few immunohistochemical stains have been described in some studies,<sup>3,4</sup> none of them is diagnostic or characteristic of CAPNONS.

The pathogenesis of CAPNON also remains unknown. Several hypotheses have been proposed, including a reactive process,<sup>2–6</sup> degenerative process,<sup>10</sup> metabolic dysfunction,<sup>11</sup> metaplastic transformation,<sup>12</sup> and neoplasm.<sup>1</sup> The hypothesis of a reactive process associated with inflammation and/or injury has been favored,<sup>3,4</sup> but there are no observational studies to support it. The most distinguishing feature of CAPNON is its granular amorphous cores that represent varying degrees of calcification/ossification over time. It is unclear what constitutes these cores. Also, it is unclear why CAPNON is located specifically in the “neuraxis” despite its predominantly mesenchymal features. The objectives of our present study were to answer these questions and identify immunohistochemical markers that could be used to diagnose CAPNON and examine its pathogenesis.

## MATERIALS AND METHODS

### Participants

Ethics approval was granted by the Hamilton Integrated Research Ethics Board. All participants gave informed consent for the research project. We retrospectively examined CAPNON specimens of 11 patients (median age: 60 years; 7 women, 4 men) who were diagnosed in the last 15 years from the hospitals of McMaster University (Hamilton, Ontario, Canada), University of Montreal (Montreal, Quebec, Canada), and Western University (London, Ontario, Canada). The diagnosis of CAPNONS was made by pathological examination revealing the characteristic histopathological features (described in Introduction) and excluding other disease entities by histopathology and immunohistochemistry (IHC).<sup>3,4,6,7</sup>

For comparison, we also examined the specimens of the following groups: intervertebral disc disease from 7 patients (median age: 68 years; 4 women, 3 men), hippocampal sclerosis (International League Against Epilepsy or ILAE type 1) from 16 patients (median age: 28 years; 4 women, 12 men), and null-cell pituitary adenoma (a neuroendocrine tumor) from 8 patients (median age: 62.5 years; 6 women, 2 men). These comparison groups were chosen, because the tissue of intervertebral disc disease and CAPNON shared some similar histological features such as calcification/ossification; CAPNONS contained inflammatory cell infiltrates, reminiscent of the immune cell infiltrates in hippocampal sclerosis the pathogenesis of which may involve an autoimmune process<sup>13</sup>; null-cell pituitary adenomas also contained immune cell infiltrates,<sup>14</sup> and possibly as well neurofilaments that were found in some other neuroendocrine tumors, which were described and discussed later in this study.

### Histopathology and Immuno Histochemistry

The surgical resection or biopsy specimens were formalin fixed, routinely processed, paraffin-embedded, sectioned at

5  $\mu$ m, and stained with hematoxylin and eosin (H&E) and by IHC. The H&E-stained slides were examined for histopathological features. Automated IHC was performed on tissue sections using the Dako Autostainer Link 48 and visualized with the Dako Envision Flex kit detection system (Dako, Carpinteria, CA, USA). Antibodies to the following were used: Neurofilament-light (NF-L; 2F11, Dako), Neurofilament-phosphorylated (NF-p; SMI 31, Covance, Berkeley, CA, USA), CD68 (KP1, Dako), CD8 (C8/144B, Dako), CD4 (4B12, Dako), glial fibrillary acidic protein (Z0334, Dako), Vimentin (V9, Dako), Desmin (D33, Dako), epithelial membrane antigen (E29, Dako), and synaptophysin (27G12, Leica). The antibodies listed here were only those immunostains described later in this study, while a few other immunostains and histological stains were also performed for the diagnosis of CAPNON in most cases.<sup>3,4</sup>

### Electron Microscopy

In three selected cases of CAPNONS, a small portion of the tissue was fixed in 2% glutaraldehyde, postfixed in 1% osmium tetroxide, dehydrated, and embedded in resin. Ultrathin sections were stained with uranyl acetate followed by lead citrate and examined with JEOL 1230 Transmission electron microscope (EM).

### Immuno Histochemical Assessment

Immunohistochemical features of each case/section were reviewed and assessed. The positivity of NF-L and NF-p was scored using the following scheme: -, absent (except linear positivity of entrapped axons); +, <10%; ++, 10%–50%; +++, > 50% within the lesion cores. This IHC was not assessed in the control group of hippocampal sclerosis, ILAE type 1 or the control group of null-cell pituitary adenoma, due to the innate neurofilament (NF) positivity in the brain and posterior pituitary.<sup>13,14</sup> The numbers of CD8+ cytotoxic T-cells and CD4+ T-cells were consistently counted in microscopic high-power fields (HPF, original magnification  $\times$  400), and the values represented sums of 10 consecutive HPFs in an area with the most frequent positive cells.

### Statistical Analysis

Nonparametric statistical analysis was performed using GraphPad Prism 8 software. The 2-tailed Mann–Whitney *U*-test was used for comparisons between the groups of CAPNONS and one of the other diseases. *P* values < 0.05 were regarded as being statistically significant.

## RESULTS

All 11 CAPNONS exhibited the characteristic histopathological features (described in Introduction) that were diagnostic of CAPNON (Figures 1A–C, and 2A). The clinical and pathological characteristics of these patients were summarized in Table 1.

### Ultrastructural Features of CAPNON

EM in three representative cases (Cases 1, 2, and 6 in Table 1) revealed that the CAPNON cores contained fibrillary materials, mostly ranging from 8 to 13 nm in diameter with the average of about 10 nm (Figure 1D), morphologically consistent with NFs.

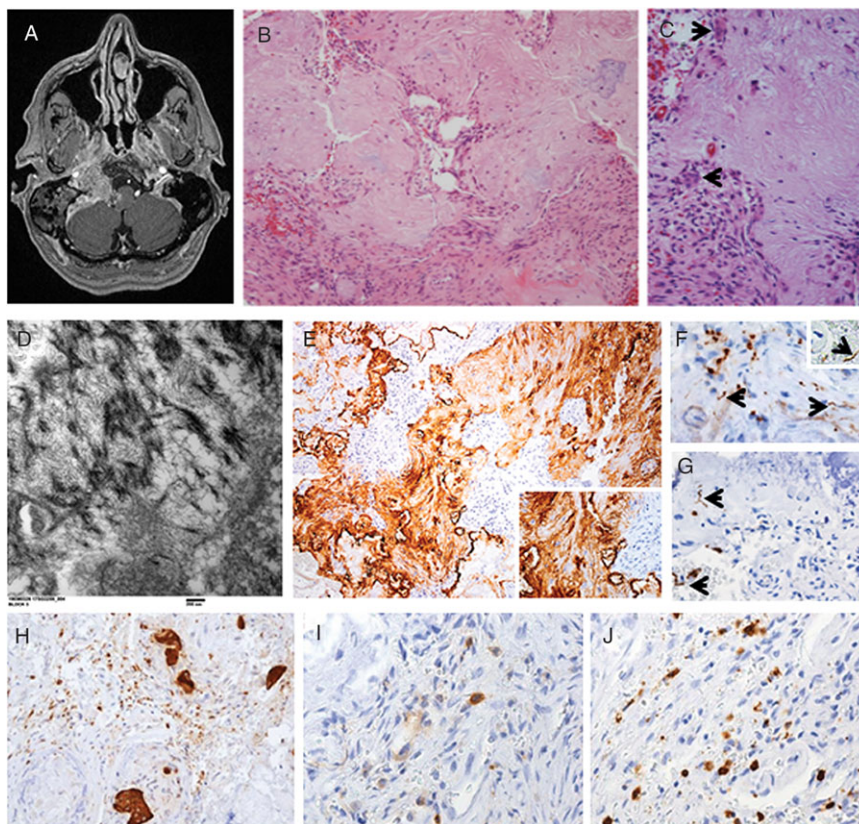


**Figure 1:** CAPNON magnetic resonance imaging and pathology. Head T1-weighted image with contrast shows a hypointense, focally calcified, enhancing lesion in the right cerebellopontine angle (A). The lesion exhibits amorphous to fibrillary cores, peripheral palisading cells, calcification/ossification (B), and multinucleated giant cells (C, arrows). Electron microscopy reveals the lesion cores containing fibrillary materials consistent with neurofilaments (D). The lesion cores demonstrate positive neurofilament-light (NF-L) immunostaining (E, F, with an inset of higher magnification) and negative neurofilament-phosphorylated (NF-p) immunostaining except occasional peripherally-located entrapped axons (G, arrows, versus F, arrows). The lesion contains focally scattered CD68+ macrophages (H), rare CD4+ T-cells (I), and focally frequent CD8+ T-cells (J). Original magnification,  $\times 100$  (B),  $\times 200$  (C, E, H–J),  $\times 400$  (F, G), and  $\times 50,000$  (D).

### Neurofilament Positivity in CAPNON

To investigate the EM finding of fibrillary materials, we performed IHC with NF and other antibodies. NF-L was positive in the cores of all 11 CAPNON cases (Figures 1E, and 2A; Table 1); in comparison, no NF-L positivity was found in seven cases of intervertebral disc disease tissues (Table 1; Figure 2D). To further delineate the NF subunit in CAPNONs, we also examined NF-p IHC in four representative cases (Table 1). There was no NF-p positivity in the CAPNON cores, but the periphery of CAPNON lesions exhibited occasional NF-p+ and NF-L+ entrapped axons (Figure 1G versus 1F). The CAPNON cores stained negative for the other intermediate filaments, including glial fibrillary acidic protein, vimentin, desmin, and synaptophysin (not shown) in several representative cases. Epithelial membrane antigen immunostaining was limited at the periphery (likely due to the leptomeningeal involvement) or completely negative in these CAPNONs, consistent with our previous reviews.<sup>3,4</sup>

### T-cell Infiltrates in CAPNON

Given the reported autoimmunity to NF-L<sup>15,16</sup> and comorbidity of CAPNON and immune-mediated diseases in at least

two patients of this series (Cases 6 and 7 in Table 1), we further examined immune cell infiltrates in 11 cases of CAPNONs. All CAPNONs showed some CD68+ macrophages, and variable infiltration of CD8+ cytotoxic T-cells with rare to no CD4+ T-cells (Figures 1H–J, 2A–C, and 3).

The amount of CD4+/CD8+ T-cells within CAPNONs was quantified and compared to that of intervertebral disc, hippocampal sclerosis ILAE type 1, and null-cell pituitary adenoma. The infiltration of CD8+ T-cells was significantly greater in the group of 11 CAPNONs than that of 7 intervertebral disc disease tissues ( $p < 0.0001$ ; Figure 2D versus 2A, and 2F versus 2C), and that of 8 null-cell pituitary adenomas ( $p = 0.0002$ ; Figure 2J versus 2A, and 2L versus 2C), but not significantly different from that of 16 intra-axial lesions of hippocampal sclerosis ILAE type 1 ( $p = 0.05$ ; Figure 2G versus 2A, and 2I versus 2C). There was no significant difference ( $p > 0.05$ ) in the infiltration of CD4+ T-cells between the groups of CAPNONs and any one of the other diseases (Figure 2E, H, K versus 2B). While the ratio of CD4+/CD8+ T-cells is normally greater than 1.5 in the blood<sup>17</sup> and higher in the brain tissue,<sup>18</sup> this ratio in the group of CAPNONs (median: 0.066) was significantly lower than that in the group of null-cell pituitary adenomas (median: 3.214;



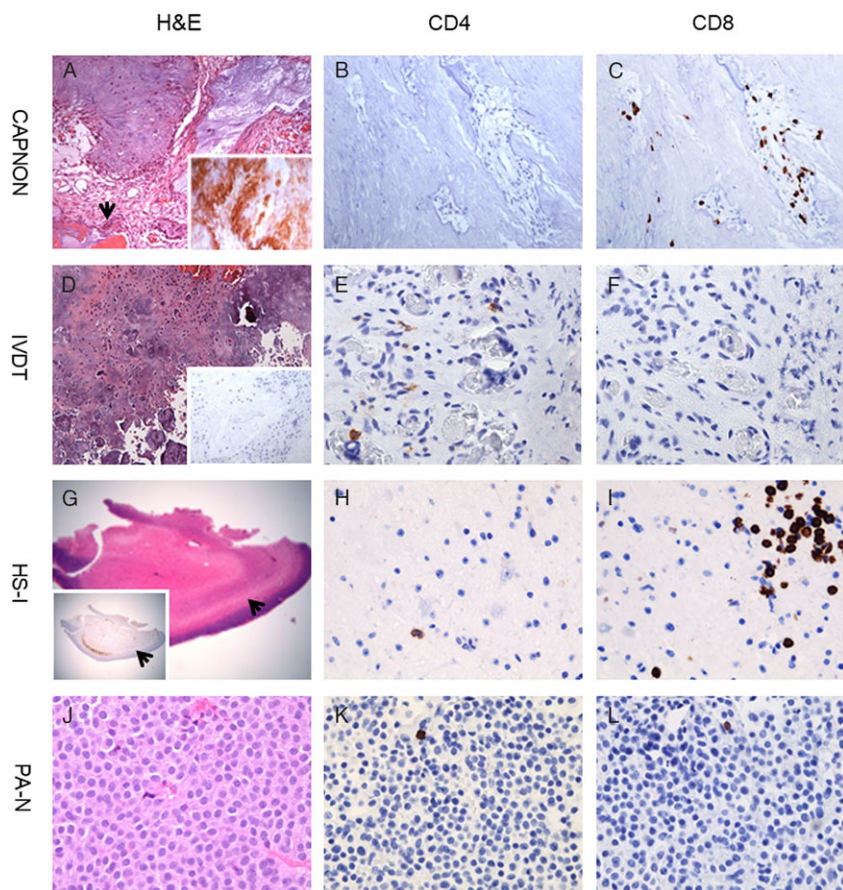


**Figure 2:** T-cells in CAPNON and other diseases. CAPNON (A) with positive neurofilament-light immunostaining (inset in A) shows no to rare CD4+ T-cells (B) and focally frequent CD8+ T-cells (C). IVDT (D) with negative neurofilament-light immunostaining (inset in D) exhibits rare CD4+ T-cells (E) and no CD8+ T-cells (F). HS-I (G) with Neu-N immunostain demonstrating neuronal loss in the hippocampus CA1 subfield (arrows; inset in G) demonstrates rare CD4+ T-cells (H) and focally frequent CD8+ T-cells (I). PA-N (J) shows rare CD4+ T-cells (K) and CD8+ T-cells (L). Original magnification,  $\times 15$  (G),  $\times 100$  (D),  $\times 200$  (A), and  $\times 400$  (B, C, E, F, H, I, J–L). CAPNON, calcifying pseudoneoplasm of the neuraxis; HS-I, hippocampal sclerosis ILAE type 1; IVDT, intervertebral disc disease tissue; PA-N, null-cell pituitary adenoma.

$p < 0.0001$ ), but not significantly different from that in the group of hippocampal sclerosis ILAE type 1 (median: 0.085;  $p = 0.584$ ; Figure 3). This suggests that CAPNON, like hippocampal sclerosis ILAE type 1, may be an immune-mediated process.<sup>13</sup>

## DISCUSSION

Our present work is one of the largest CAPNON case series published to date, and the first case–control/observational study to examine biomarkers in the diagnosis and pathogenesis of CAPNON. This study provides several novel observations, including the aggregation of NF-L in the CAPNON granular amorphous cores, entrapment of the axons at the CAPNON periphery, and the infiltration of CD8+ cytotoxic T-cells with a decreased ratio of CD4/CD8+ T-cells in CAPNONs. Our findings suggest that IHC of NF-L and CD4/CD8+ may serve as the markers to diagnose CAPNON in clinical/pathological practice and investigate the pathogenesis of CAPNON.

NF is a neuronal cytoplasmic protein highly expressed in axons, where they contribute to the cytoskeleton and facilitate

axonal transport.<sup>15,16,19,20</sup> Mammalian NF is composed of three major subunits based on their molecular weight: NF-light (NF-L, ~70 kDa), medium (NF-M, ~160 kDa), and heavy (NF-H, ~200 kDa, or NF-p). The levels of NF-L increase in cerebrospinal fluid and blood proportionally to the degree of axonal damage in a variety of neurological disorders, including inflammatory, neurodegenerative, traumatic, and cerebrovascular diseases. Therefore, NF-L has been considered as a promising diagnostic and prognostic biomarker of axonal damage in these neurological diseases.<sup>19,20</sup> NF-L corresponds to the IHC 2F11 antibody, directed against ~70 kDa protein.<sup>21,22</sup> In our present study, the finding of NF-L (rather than NF-p) in all CAPNON cores indicates that CAPNONs contain NF-L, and suggests that IHC with NF-L can aid the diagnosis of CAPNONs, along with histological examination.

The IHC positivity of NF-L is also seen in neuroendocrine tumors in a few sites including cutaneous tissue, gastrointestinal tract, breast, lung, and mediastinum,<sup>23–25</sup> as well as the testis and testicular germ-cell tumors.<sup>22</sup> The presence of NF-L in the testis and testicular germ-cell tumors has been attributed to the

**Table 1: Clinical and pathological characteristics of participants**

Case	Age (yrs), Sex	Clinical presentation	History/ Comorbidity	Location	Imaging	Surgery/ Treatment	Pathology Diagnosis	IHC NF-L	IHC NF-p	Follow-up
1	57, M	Hoarseness, dysphagia, Ataxia × 2 mos	Diffuse right mastoid effusion	Right cerebello pontine angle	CT: heavily calcified lesion; MRI: a 3.5 × 2.1 × 2.0 cm lesion, hypointense on T1WI, isointense on T2WI, with avid contrast enhancement	STR	CAPNON	+++	-	Stable at 15 mos
2	70, M	Headache, cognitive Impairment × 4 yrs	Remote West Nile virus encephalitis, seizures, hypertension, obstructive sleep apnea	Right anterior skull base	CT: a 2.4 × 2.6 × 1.8 cm well-circumscribed, lobulated, densely calcified lesion; MRI: hypointense on both T1WI and T2WI, with patchy central T2 hyperintensity, and peripheral contrast enhancement	Near-total resection	CAPNON	+++	-	No lesion progression on imaging at 7 yrs; progressive global neurological decline, but without focal neurologic deficits
3	64, F	Incidental finding at surgery for other medical conditions	Ruptured aneurysm with recurrent subarachnoid hemorrhage and intraventricular hemorrhage, hypothyroidism	Inner aspect of the dura covering the right cerebrum, numerous nodules	CT: calcified nodules; 2–4 mm in maximal dimension; MRI: centrally hypointense and peripherally hyperintense on T2WI	GTA	CAPNON	++	ND	No recurrence of resected lesion at 2 mos; stable other lesions
4	64, F	Left-sided neck pain × 2 yrs, following a fall and C2-C5 fracture	Arthritis, cervical cancer	C2-4 epidural	CT+MRI: destructive expansile and sclerotic lesion with a cystic area, calcification, and heterogeneous contrast enhancement	Resection, not specified	CAPNON	+++	ND	Stable at 2 yrs, despite another operation of C2-C5 posterior instrumented fusion and resection of lateral mass at 14 mos
5	60, M	Progressive cervical myelopathy × 3 weeks to few mos	Hypertension, cataract extraction, kidney stone removal	C7 epidural	MRI: a large compressive lesion, measuring 13.9 × 9.5 × 6.18 mm, isointense on T1WI and T2WI; another hypointense, calcified mass, measuring 17.3 × 10.9 × 8.5 mm	Resection, not specified	CAPNON	+++	ND	Stable at 7 mos; improved myelopathy
6	51, F	Lower back pain × 2 yrs	Systemic lupus erythematosus, end-stage renal disease on dialysis, scleroderma with associated interstitial lung disease, hypertension, glomerulonephritis, anemia	L3-4 epidural to paraspinal	MRI: midline mass, 5.9 × 3.6 × 5 cm, centered in the deep subcutaneous tissue/fascia at L3-L4, with extensive calcification, and invasion into the spinous process at the level of L3 and left paravertebral muscle	Biopsy	CAPNON	+++	ND	Stable at 2 mos
7	64, F	left lower back pain × 6 mos	Autoimmune hepatitis, type 2 diabetes mellitus, hypertension, osteoporosis	L5-S1 epidural	CT: a lobulated, calcified mass, 3.8 × 1.3 × 2.2 cm, along the left side of the L5-S1 spinal canal. MRI: signal void on T2WI, and hypointense on T1WI	Resection, not specified	CAPNON	++	-	Complete resolution of neurologic symptoms, and MRI showing no recurrence at 6 mos

**Table 1.** *Continued*

Case	Age (yrs), Sex	Clinical presentation	History/ Comorbidity	Location	Imaging	Surgery/ Treatment	Pathology Diagnosis	IHC NF-L	IHC NF-p	Follow-up
8	42, M	Episodes of right lower limb weakness and right leg clonus × 1 yr; constant vertex headache × 2 mos	Agenesis of corpus callosum on imaging	Cingulate gyri and corpus callosum	MRI: large midline fronto-parietal heavily calcified heterogenous lesion with cystic and fat components with contrast enhanced areas; hyperintensity on T2WI and FLAIR of the right and left fronto-parietal surrounding white matter suggestive of gliosis or vasogenic edema	Partial resection	CAPNON	+++	ND	Partial seizures 1 yr later; gradual slow cognitive deterioration at 10 yrs
9	56, F	Simple partial seizure of left upper limb × 1 mo; mild weakness of left upper limb	Not documented	Right fronto-parietal lobe	MRI: 2 cm fronto-parietal calcified lesion, hypointense on T1WI and T2WI, with contrast enhancement; hyperintense on T2WI of the surrounding white matter suggestive of vasogenic edema	Partial resection	CAPNON	+++	ND	No weakness at 1 yr; no lesion recurrence at 2 yrs
10	48, F	Worsening headache × yrs, especially right frontal region	Migraines × yrs	Right frontal lobe	MRI: 9 × 10 mm right frontal subcortical, centrally calcified lesion with peripheral contrast enhancement; hyperintensity on T2WI of the surrounding tissue extending to the frontal horn suggestive of vasogenic edema; mild increase in size from 6.5 mm to 10 mm in 2 yrs	Partial resection	CAPNON	++	ND	No post-operative deficit; no lesion recurrence at 8 yrs
11	70, F	Migraines × yrs	Two motor vehicles accidents 28 yrs and 6 yrs earlier, with no recognized craniocerebral injury on either occasion	Right frontal lobe	MRI: a heterogeneous intra-axial mass with central cystic areas, hypointensities on T1WI and T2WI, central calcification, peri-lesional edema, intense heterogeneous ring and intra-lesional contrast enhancement; 3 × 2 × 2 cm at operation	Resection, not specified	CAPNON	+++	-	Stable at 2 yrs
12–19 Age: range, 53–75 yrs; median, 68 yrs; 4 F, and 3 M							IVDT	-	ND	
20–35 Age: range, 4–59 yrs; median, 28 yrs; 4 F, and 12 M (Reference, 13)							HS-I	N/A	N/A	
36–43 Age: range, 34–77 yrs; median, 62.5 yrs; 6 F, and 2 M (Reference, 14)							PA-N	N/A	N/A	

Abbreviations: CAPNON, Calcifying pseudoneoplasm of the neuraxis; CT, computed tomography; F, female; HS-I, hippocampal sclerosis, type I; GTR, gross total resection; IHC, immunohistochemistry; IVDT, intervertebral disc disease tissue; M, male; mos, months; MRI, magnetic resonance imaging; ND, not done; N/A, not applicable; PA-N, pituitary adenomas, null cell; T1WI, T1-weighted imaging; T2WI, T2-weighted imaging; yrs, years.

IHC NF-L/NF-p: -, absent (except linear positivity of peripherally-located entrapped axons); +, < 10%; ++, 10–50%; +++, > 50% of the lesion cores.

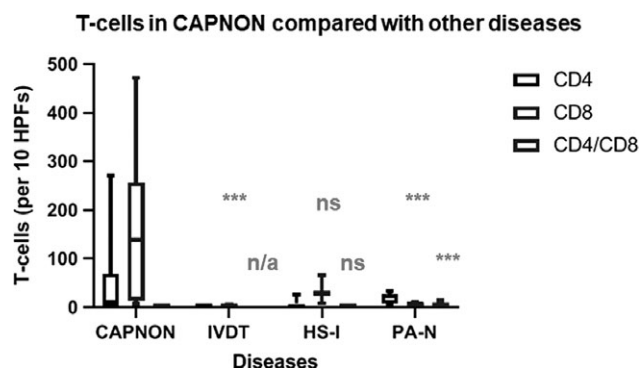


**Figure 3:** T-cells in CAPNON compared with other diseases. CAPNONs (n = 11) show significantly more CD8<sup>+</sup> T-cells with less CD4<sup>+</sup> T-cells and a decreased CD4/CD8<sup>+</sup> ratio, compared with IVDT (intervertebral disc disease tissue; n = 7), HS-I (hippocampal sclerosis, ILAE type 1; n = 16) and PA-N (null-cell pituitary adenoma; n = 8). In the box graphs, values represent the median and 25/75 percentile, with the horizontal lines inside each box indicating the median and whiskers demonstrating 5/95 percentile, from the patients in each group. \*\*\*, p < 0.001 (versus CAPNONs) by the 2-tailed Mann–Whitney U-test; ns, not significant (versus CAPNONs); n/a, not applicable (because of 0 in some IVDT cases).

involvement of neural tissue.<sup>22</sup> Our present study has identified NF-L+ (and NF-p+) entrapped axons at the periphery of CAPNONs, in addition to the aggregation of NF-L in the CAPNON cores, which supports the involvement of neural tissue in the formation of CAPNONs. In the neuraxis, CAPNONs can occur either in the central nervous system (intra-axial, brain, or spinal cord parenchymal tissue) or peripheral nervous system (extra-axial, nerves), and their occurrence may be associated with preferential entrapment of the adjacent neural tissue that is presumably the source of NF-L in CAPNONs. In extra-axial CAPNONs, there are NF-L debris and fragmented axons that may be identified at the lesion periphery (as demonstrated in Figure 1F). The CAPNON cores could be formed with the aggregation of tissue debris containing NF-L from the damaged axons, which then calcify or ossify over time; and the surrounding tissue components of CAPNONs are likely reactive in nature. This hypothesis of CAPNON formation due to axonal entrapment from the adjacent neural tissue may explain the specific location of “neuraxis” for CAPNON.

The clinical manifestations of CAPNONs may be highly variable, ranging from a subclinical lesion found incidentally on pathological examination to marked tumor-like mass effect, mainly depending on the lesion location, size, and comorbidity (Table 1).<sup>1–9</sup> Intracranial CAPNONs most commonly manifest with headaches and/or seizures (in approximately 1/3 of the cases) due to the localized mass effect.<sup>2</sup> Incidental CAPNONs are not very uncommon, especially when they occur in association with other lesions including tumors.<sup>1,4</sup> CAPNONs have been also occasionally reported in collision with tumors such as dysembryoplastic neuroepithelial tumor, low-grade gliomas, meningioma, and lipomas, as well as rheumatoid nodules.<sup>28</sup> In these cases of CAPNONs with coexisting or collision lesions, the presentation of CAPNONs may be overwhelmed by that of the other lesions.

Although the pathogenesis of CAPNON needs further investigation, we propose an autoimmune-mediated process in the

pathogenesis of CAPNONs, based on the following observations: (i) our findings of CD8<sup>+</sup> cytotoxic T-cell infiltration with a decreased ratio of CD4/CD8<sup>+</sup> T-cells;<sup>17,18</sup> (ii) no difference in the infiltration of CD8<sup>+</sup> cytotoxic T-cells or the CD4/CD8<sup>+</sup> ratio between the specimens of CAPNONs and hippocampal sclerosis ILAE type 1, likely an autoimmune process<sup>13</sup>; (iii) CAPNONs containing NF-L, an autoimmune target identified in several neurological diseases, and the aggregation of NF-L likely associated with an autoimmune process in CAPNONs.<sup>15,16</sup> A recent case report showed a high ratio of infiltrating M2 (CD163+, alternatively activated)/M1 (CD68+/IBA1+, classically activated) macrophages and a high uptake of 11C-methionine positron emission tomography in an intra-axial CAPNON associated with an adjacent lipoma and agenesis of the corpus callosum, supportive of an activated immune response.<sup>26</sup> We also reported a similar case (case 8 in Table 1) with immune cell infiltrates and inflammatory response.<sup>27</sup> Another recent case report from our team demonstrated collision lesions of CAPNON and rheumatoid nodules in a patient with systemic lupus erythematosus (an autoimmune disease; case 6 in Table 1) as well as transitional lesions from rheumatoid nodules to CAPNON lesions.<sup>28</sup> These case reports further support our hypothesis of an immune-mediated process in CAPNONs.

The limitations of our present study include the lack of molecular studies such as the western blotting to confirm the presence of NF-L corresponding to IHC in CAPNONs. As the preoperative diagnosis of CAPNONs was challenging, no fresh or frozen tissue had been collected from our cases of CAPNONs. Nevertheless, IHC positivity of NF-L can help with the diagnosis of CAPNON. Another limitation is the relatively small number of cases presented here partially due to the rarity and diagnostic challenges of CAPNONs. Future studies in a larger number of cases may be needed to verify our present findings in this study.

## CONCLUSION

The expression of NF-L and a decreased ratio of CD4/CD8<sup>+</sup> T-cells can aid the diagnosis of CAPNON. We propose that the pathogenesis of CAPNON is likely immune-mediated, with the aggregation of NF-L and immune cell infiltrates. Since both NF and T-cells have been considered for the therapeutic targets,<sup>19,20,29</sup> these immunohistochemical markers may not only be diagnostic but also potentially therapeutic.

## ACKNOWLEDGEMENTS

The authors thank Ms. Bruna Capretta (Hamilton General Hospital) for administrative assistance and Dr. Lee Cyn Ang (Western University) for his advice on the present study. The present study included seven case reports published by our authors,<sup>3,4,6,7,27,28</sup> and two previously published case series which served as controls for CAPNONs,<sup>13,14</sup> but there is no duplication of the principal data or demonstration between this study and our other publications.

## DISCLOSURES

The authors report no conflict of interest concerning the materials or methods used in this study or the findings specified in this paper.



## STATEMENT OF AUTHORSHIP

KY and JQL designed the study. KR, BHW, AC, JP, SP, WHY, FB, MWB, RH, and JQL provided patient data and analysis. KY and JQL extracted the data and wrote the manuscript. All authors critically reviewed and approved the final manuscript.

## REFERENCES

- Rhodes RH, Davis RL. An unusual fibro-osseous component in intracranial lesions. *Human Pathol.* 1978;9(3):309–19.
- Barber SM, Low JCM, Johns P, Rich P, MacDonald B, Jones TL. Calcifying pseudoneoplasm of the neuraxis: a case illustrating natural history over 17 years of radiologic surveillance. *World Neurosurg.* 2018;115:309–19.
- Yang K, Reddy K, Ellenbogen Y, Wang BH, Bojanowski MW, Lu JQ. Skull base calcifying pseudoneoplasms of the neuraxis: two case reports and a systematic review of the literature. *Can J Neurol Sci.* 2020;47:389–97.
- Lu JQ, Yang K, Reddy KKV, Wang BH. Incidental multifocal calcifying pseudoneoplasm of the neuraxis: case report and literature review. *Br J Neurosurg.* 2020;12:1–8.
- Ho ML, Eschbacher KL, Paolini MA, Raghunathan A. New insights into calcifying pseudoneoplasm of the neuraxis (CAPNON): a 20-year radiological-pathological study of 37 cases. *Histopathology.* 2020;76(7):1055–69.
- Kocovski L, Parasu N, Provias JP, Popovic S. Radiologic and histopathologic features of calcifying pseudoneoplasm of the neural axis. *Can Assoc Radiol J.* 2015;66(2):108–14.
- Haji F, Alturkustani M, Parrent A, Megyesi J, Gulka I, Hammond R. Simple partial seizures in a 70-year-old female. *Can J Neurol Sci.* 2011;38:507–11.
- Aiken AH, Akgun H, Tihan T, Barbaro N, Glastonbury C. Calcifying pseudoneoplasms of the neuraxis: CT, MR imaging, and histologic features. *AJNR Am J Neuroradiol.* 2009;30(6):1256–60.
- Qian J, Rubio A, Powers JM, et al. Fibro-osseous lesions of the central nervous system: report of four cases and literature review. *Am J Surg Pathol.* 1999;23(10):1270–75.
- McCarthy EF. Pseudotumors and reactive lesions. *Surg Pathol Clin.* 2012;5(1):257–86.
- Abdaljaleel M, Mazumder R, Patel CB, et al. Multiple calcifying pseudoneoplasms of the neuraxis (MCAPNON): distinct entity, CAPNON variant, or old neurocysticercosis? *Neuropathology.* 2017;37:233–40.
- Hubbard M, Qaiser R, Clark HB, Tummala R. Multiple calcifying pseudoneoplasms of the neuraxis. *Neuropathology.* 2015;35:452–55.
- Lu JQ, Steve TA, Wheatley M, Gross DW. Immune cell infiltrates in hippocampal sclerosis: correlation with neuronal loss. *J Neuropathol Exp Neurol.* 2017;76:206–15.
- Lu JQ, Adam B, Jack AS, Lam A, Broad RW, Chik CL. Immune cell infiltrates in pituitary adenomas: more macrophages in larger adenomas and more T cells in growth hormone adenomas. *Endocr Pathol.* 2015;26:263–72.
- Puentes F, van der Star BJ, Boomkamp SD, et al. Neurofilament light as an immune target for pathogenic antibodies. *Immunology.* 2017;152:580–88.
- Puentes F, van der Star BJ, Victor M, et al. Characterization of immune response to neurofilament light in experimental autoimmune encephalomyelitis. *J Neuroinflammation.* 2013;10:118.
- McBride JA, Striker R. Imbalance in the game of T cells: What can the CD4/CD8 T-cell ratio tell us about HIV and health? *PLoS Pathog.* 2017;13(11):e1006624.
- Hansen N, Schwing K, Önder D, et al. Low CSF CD4/CD8+ T-cell proportions are associated with blood-CSF barrier dysfunction in limbic encephalitis. *Epilepsy Behav.* 2020;102:106682.
- Gaetani L, Blennow K, Calabresi P, Di Filippo M, Parnetti L, Zetterberg H. Neurofilament light chain as a biomarker in neurological disorders. *J Neurol Neurosurg Psychiatry.* 2019;90:870–81.
- Khalil M, Teunissen CE, Otto M, et al. Neurofilaments as biomarkers in neurological disorders. *Nat Rev Neurol.* 2018;14:577–89.
- van Muijen GN, Ruiter DJ, van Leeuwen C, Prins FA, Rietsema K, Warnaar SO. Cytokeratin and neurofilament in lung carcinomas. *Am J Pathol.* 1984;116:363–69.
- Miettinen M, Virtanen I, Talerman A. Intermediate filament proteins in human testis and testicular germ-cell tumors. *Am J Pathol.* 1985;120:402–10.
- Astarloa R, Sánchez-Franco F, Cacicado L, García-Villanueva M. Differential expression of neurofilament triplet proteins in carcinoma tumours: an immunohistochemical study. *Br J Cancer.* 1991;63:715–18.
- Stanoszek LM, Chan MP, Palanisamy N, et al. Neurofilament is superior to cytokeratin 20 in supporting cutaneous origin for neuroendocrine carcinoma. *Histopathology.* 2019;74:504–13.
- Miettinen M, Lehto VP, Dahl D, Virtanen I. Varying expression of cytokeratin and neurofilaments in neuroendocrine tumors of human gastrointestinal tract. *Lab Invest.* 1985;52:429–36.
- Inukai M, Shibahara I, Hotta M, et al. Case of calcifying pseudoneoplasms of the neuraxis coexisting with interhemispheric lipoma and agenesis of the corpus callosum: involvement of infiltrating macrophages. *World Neurosurg.* 2020;134:635–40.
- Lu JQ, Berthelet F, Bojanowski MW. Letter to the editor regarding “Case of calcifying pseudoneoplasms of the neuraxis coexisting with interhemispheric lipoma and agenesis of the corpus callosum: involvement of infiltrating macrophages”. *World Neurosurg.* 2020;139:668–69. doi: [10.1016/j.wneu.2020.04.003](https://doi.org/10.1016/j.wneu.2020.04.003)
- Lu JQ, Popovic S, Provias J, Cenic A. Collision lesions of calcifying pseudoneoplasm of the neuraxis and rheumatoid nodules: a case report with new pathogenic insights. *Int J Surg Pathol.* 2020 Jul 15:1066896920941939. doi: [10.1177/1066896920941939](https://doi.org/10.1177/1066896920941939). Online ahead of print.
- Kallies A, Zehn D, Utzschneider DT. Precursor exhausted T cells: key to successful immunotherapy? *Nat Rev Immunol.* 2020;20:128–36.